FUDMA Journal of Sciences (FJS)
ISSN online: 2616-1370
ISSN print: 2645 - 2944
Vol. 10 No. 17, September, 2026, pp 180 – 187
DOI: https://doi.org/10.33003/fjs-2026-1017-6042

Green Synthesis of Iron Nanoparticle Catalyst Using *Manihot esculenta* (Cassava) Peels Waste Extract and Their Application for the Degradation of Pharmaceutical Wastewater

Merit Amarachukwu Eze, *Jibrin Noah Akoji and Lami Karimatu Abdullahi

Department of Chemistry, Baze University, Abuja, Nigeria.

*Corresponding authors' email: noah.akoji@bazeuniversity.edu.ng

Received: 08 Sept. 2026
Accepted: 11 Sept. 2026
Published: 23 Sept. 2026

ABSTRACT

The synthesized iron nanoparticles (FeNPs) were characterized using Scanning Electron Microscopy coupled with Energy Dispersive X-ray spectroscopy (SEM-EDX), Ultraviolet-Visible Spectroscopy (UV-Vis), X-Ray Diffraction (XRD), Thermogravimetric Analysis (TGA), Fourier Transformed Infrared Spectroscopy (FTIR) and Brunauer-Emmett-Teller (BET) analysis. In addition, environmental impact assessment was conducted through reusability tests and toxicity assessments using Clarias gariepinus and Chlorella vulgaris which revealed the low risk of the FeNPs in the environment. The BET analysis revealed that the FeNPs have a high surface area of 407.111 m^2/g, pore volume of 0.190 cm^3/g, and an average pore size of 2.398 nm indicating microporosity. The XRD analysis confirmed a stable face-centred cubic crystal structure with the UV-Vis result confirming successful formation of iron oxide nanoparticles stabilized by cassava peel phytochemicals. The SEM-EDX revealed an irregular, agglomerated and porous morphologies with iron as the dominant element, characteristic of green-synthesized iron nanoparticles. FTIR analysis showed the presence of bioactive compounds which confirms that cassava peel extract served dual functions as both a reducing and stabilizing agent while TGA confirms thermal stability up to 400^0C. The synthesized FeNPs showed remarkable catalytic activity achieving an 88% degradation of paracetamol and 83% of ampicillin under optimized conditions of pH 5 and temperature 80^0C. These findings have added value to the existing research in the field of green nanotechnology and contributes to developing safer alternatives in pharmaceutical wastewater treatment, providing environmentally friendly agricultural practices while protecting human health and ecosystems.

Keywords: Green Synthesis, Iron Nanoparticles, *Manihot esculenta*, Pharmaceutical Wastewater, Photocatalytic Degradation

INTRODUCTION

Pollution remains a pressing and devastating environmental challenge generated by increased human activity in the 21st century, which poses severe threats to human life, ecosystems, and the planets at large (OECD, 2019). As industrialization, urbanization, and population growth continue to increase, the release of harmful substances into the air, water, and soil has significantly altered the natural balance of the environment. This research is important because it seeks to explore a new and environmentally friendly way of treating pharmaceutical wastewater using green iron nanoparticles synthesized from cassava peel.

In recent years, the environmental impact of pharmaceutical effluents has become an increasingly urgent concern, particularly as the global demand for pharmaceuticals continues to rise. Pharmaceutical pollution, often overlooked in broader environmental discussions, poses significant threats to ecological integrity and public health. Effluents from pharmaceutical industries, comprising active pharmaceutical ingredients (APIs), solvents, heavy metals, and other chemical by-products are frequently discharged into water bodies and surrounding land with inadequate treatment or monitoring (Kayode-Afolayan *et al*., 2022). These substances are biologically active, persistent, and capable of exerting toxic effects even at low concentrations.

The aim of this study is to develop a green synthesis method for the degradation of pharmaceutical waste using iron nanoparticles synthesized from *Manihot esculenta* peel extract while also reducing the amount of peel in the environment.

MATERIALS AND METHODS

This study employs an experimental laboratory research design to synthesize iron-based nanoparticles (FeNPs) using *Manihot esculenta* (cassava) peel extract, characterize them, and evaluate their efficiency in the degradation of selected pharmaceutical wastes (Ampicillin and Paracetamol).

Sample Collection and Identification

Cassava peels were collected from a local cassava processing site in Gwagwalada, Abuja Nigeria. The latitude and longitude for Gwagwalada, Abuja (Federal Capital Territory), Nigeria are approximately 8.95080N and 7.07670E respectively. The plant was identified as Manihot esculenta Crantz with the voucher number; BUH 10000119.

Preparation of Cassava Peel Extract

About 50 g of fresh cassava peels were thoroughly washed with tap water followed by distilled water to remove dirt and surface impurities. They were then air-dried at room temperature (30ºC) for 7 days. When a constant weight was achieved, the dried peels were ground into fine powder using a clean mechanical grinder.

For extract preparation, the cassava peel extract was prepared using a solid-to-solvent ratio of 30 g:200 mL (0.15 g/mL; 1:6.67 w/v). Approximately 30 g of the cassava peel powder obtained was added to 200 mL of distilled water in a beaker

and heated at 80°C for 30 minutes under continuous stirring. The resulting mixture was allowed to cool to room temperature of 27ºC and then filtered using Whatman No.1 filter paper. The filtrate (cassava peel aqueous extract) was stored at 4°C in refrigerator for further use for nanoparticle synthesis.

Green Synthesis of Iron Nanoparticles

A 2:1 solvent to extract ratio was used. Exactly 100 mL of 0.1 M $FeCl_2.4H_20$ (198.81 g/mol) solution was slowly added dropwise to 50 mL of cassava peel extract in a 250 mL Erlenmeyer flask. The reaction mixture was stirred continuously at room temperature (30ºC). The reaction mixture was observed for any color change, which indicated the formation of iron nanoparticles. A visible color change from light yellow to dark brown indicated the formation of iron nanoparticles. The formation was further confirmed by UV-Vis spectroscopy.

The reaction was allowed to proceed for 24 hours to ensure complete reduction of Fe^{2+} ions. The resulting colloidal solution containing FeNPs was separated by centrifugation at 10,000 rpm for 15 minutes, washed twice with distilled water and ethanol to remove impurities or any unreacted biological materials, and dried at 60 °C in a hot air oven. The dried FeNPs were stored in airtight containers for further characterization and application studies.

Characterization of FeNPs

The synthesised FeNPs were characterized using, UV-Vis (Agilent Cary 3500 Flexible UV-Vis.), FTIR (Bruker VERTEX NEO R.), SEM-EDX (Zeiss Gemini 1 -Sigma 300)., XRD (ARL'XTRA with serial number 19492086), TGA (PerkinElmer TGA 4000) and BET (Nova 4200e).

Degradation Experiments

1. A batch experiment was conducted by adding 50 mg of FeNPs to 100 mL of pharmaceutical waste solution.
2. The pH was adjusted (pH 7).
3. The mixture was agitated
4. At predetermined intervals (0, 15, 30, 60 and 90 minutes), aliquots were withdrawn, centrifuged, and analyzed.

Ecotoxicity Assessment Using Fish Fingerlings and Algae

Fish acute toxicity was evaluated following OECD Test Guideline 203, while algal growth inhibition was assessed according to OECD Test Guideline 201 guidelines developed by the Organisation for Economic Co-operation and Development (OECD, 2019). Fish fingerlings: *Clarias gariepinus* (African catfish)

i. Algae: *Chlorella vulgaris*

These organisms represent higher consumers (fish) and primary producers (algae) in the aquatic ecosystem.

Collection and Acclimatization of Test Organisms

a. Fish Fingerlings

Healthy fingerlings of 3-week-old (3-6 cm length) were obtained from a local fish hatchery. The fish were acclimatized in clean, dechlorinated water for 2 days before testing. While the water containing the algae was changed 24 hours before the start of the analysis.

Exposure and Observation (Static or Semi-Static) Fingerlings

To achieve this, beakers were used with each containing 5 fish fingerlings. The test duration was 48 hours with no feeding to avoid confounding effects.

i. Control- water only (no toxicant)

ii. Test concentrations- Different concentrations (25 and 50) % for the two simulated pharmaceutical wastewater. Fish were transferred into the beakers and observed for 48 hours.

b. Algal Culture

To preparation the test solutions, wastewater was diluted with clean water to prepare 0% (Control), 25% and 50% concentrations of the pharmaceutical wastewater.

The algae (initial density: ~1 × 10^4 cells/mL) were inoculated into beakers containing different concentrations

Test duration: 24 hours.

RESULTS AND DISCUSSION

Characterisation

The FTIR spectrum of the synthesized FeNPs was shown in figure 1. The FeNPs exhibited a broad absorption band at approximately 3339 cm^{-1}, attributed to O-H stretching vibrations of surface hydroxyl groups and adsorbed water molecules. The peak at 2922 cm^{-1} corresponds to aliphatic C-H stretching vibrations, indicating the presence of organic residues or stabilizing agents. Such broad O-H bands are commonly reported in plant-mediated nanoparticle synthesis due to the presence of polyphenols and flavonoids that act as reducing agents (Eche *et al*., 2025). Similar observations were reported for green-synthesized iron nanoparticles where hydroxyl groups were responsible for metal ion reduction (Singh *et al*., 2018).

From Plate 1, the SEM micrographs (at 50, 100, and 200 µm scales) revealed that the synthesized iron nanoparticles exhibit irregular, non-uniform, and agglomerated morphology which are characteristics of green-synthesized iron nanoparticles. The EDX analysis in figure 2 confirmed the predominance of iron with strong Fe peaks around 6.4-7.0 keV, accompanied by oxygen, indicating the formation of iron oxide species. The observed morphology and elemental composition are consistent with previous reports on plant-mediated iron nanoparticle synthesis (Singh *et al*., 2018).

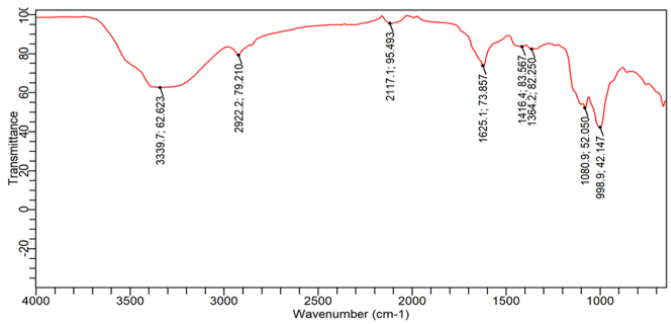

Figure 1: FTIR Spectra of the Synthesized Iron Nanoparticle

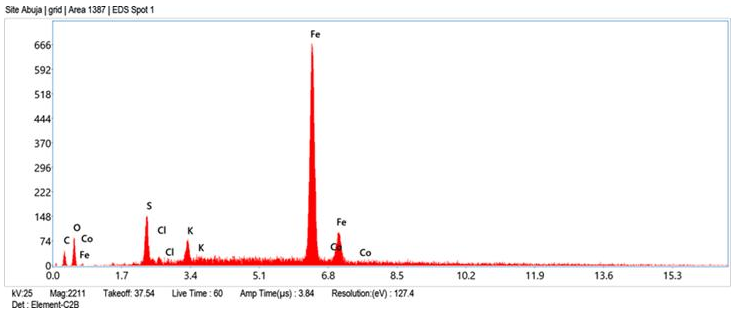

Figure 2: EDX (Energy Dispersive X-ray Spectroscopy

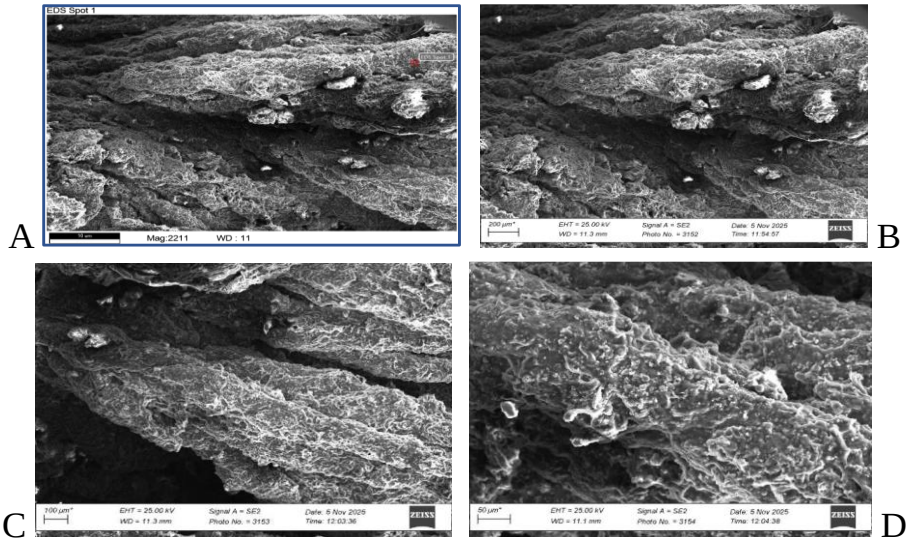

Plate1 (a-d): SEM (Scanning Electron Microscopy) Analysis of Iron Nanoparticles Synthesized from Cassava Peels

From figure 3, the spectrum showed that the XRD pattern of the iron nanoparticles synthesized from cassava peel extract revealed hematite (α-Fe_2O_3) as a major crystalline phase and marcasite as the dominant phase which is consistent with numerous recent studies on plant-mediated iron nanoparticle synthesis (Khan & Khan, 2022).

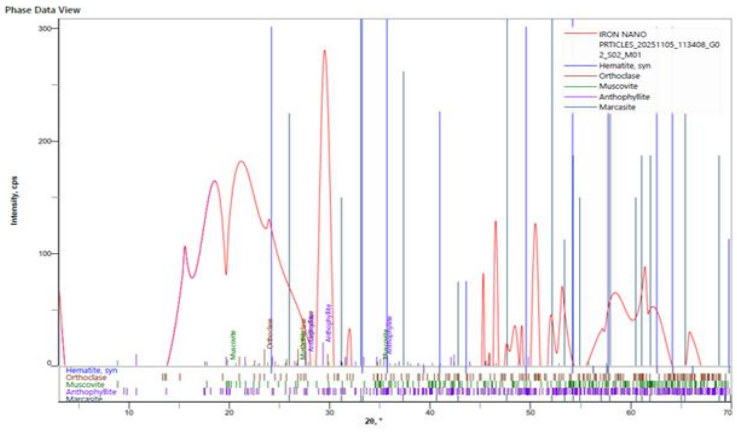

Figure 3: XRD (X-Ray Diffraction) Analysis of Iron Nanoparticles Synthesized from Cassava Peels

The average crystallite size of the synthesized iron nanoparticles was estimated using the Scherrer equation, $D=K\lambda/\beta\cos\theta$, where K=0.9, λ=0.15406 nm (Cu Kα radiation), β is the full width at half maximum (FWHM) in radians, and θ is the Bragg angle. Using the principal diffraction peak at $2\theta=29.72^0$ with an FWHM of 0.70^0, the crystallite size was calculated to be 11.74 nm. The peak positions and crystallinity observed in this study closely resemble those reported by (Singh *et al.*, 2022) who obtained hematite nanoparticles within the nanoscale range (15-45 nm) for environmental remediation applications**.**

DTG (Derivative Thermogravimetry)

From figure 4, a pronounced and sharp weight loss occurs between approximately 250 °C and 380 °C, as clearly shown by the steep decline in the TGA curve and the strong DTG peak centered around 320-340 °C. This major degradation stage corresponds to the thermal decomposition of organic

compounds from the cassava peel extract that served as reducing and stabilizing agents during synthesis. These organic constituents include polyphenols, flavonoids, carbohydrates, and residual starch components, which undergo carbonization and breakdown at elevated temperatures. The substantial mass loss in this temperature region confirms successful phytochemical capping of the nanoparticles (Kumar *et al*., 2023).

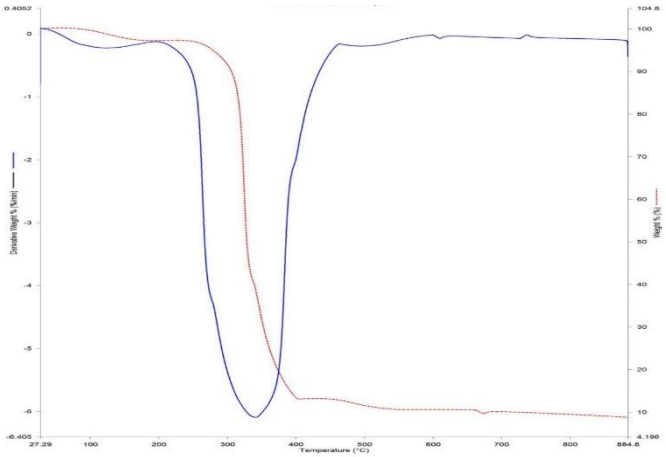

Figure 4: TGA (Thermogravimetric Analysis) Analysis of Iron Nanoparticles Synthesized from Cassava Peels

UV–Visible Spectroscopic

From figure 5, the UV-Vis spectrum exhibited a strong absorption band around 260 nm, which confirms the successful synthesis of well-dispersed iron nanoparticles with strong UV absorption properties, supporting their suitability for catalytic degradation of pharmaceutical wastewater.

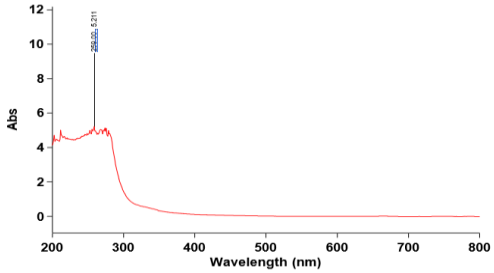

Figure 5: UV-VIS Analysis of Iron Nanoparticles Synthesized from Cassava Peels

BET (Brunauer–Emmett–Teller Characterization

The cumulative pore volume analysis in figure 6 revealed a gradual increase in pore volume with increasing pore diameter, reaching a total pore volume of approximately 0.190 cm^3/g. According to the IUPAC classification of adsorption-desorption isotherms, the nitrogen adsorption-desorption isotherm was of Type IV isotherm with an H3 hysteresis loop, which confirms the presence of mesopores in the iron nanoparticles synthesized. These nanoparticles possessed a very high surface area of 407.111 m^2/g and an average pore size of 2.398 nm. The majority of the pore volume was contributed by pores within the 1.8-2.5 nm range, indicating the dominance of small mesopores with minor microporous features. Combined with the BJH pore size distribution, the synthesized iron nanoparticles can be classified as predominantly mesoporous based on the IUPAC classification (2-50nm) which is suitable for adsorption and catalytic degradation.

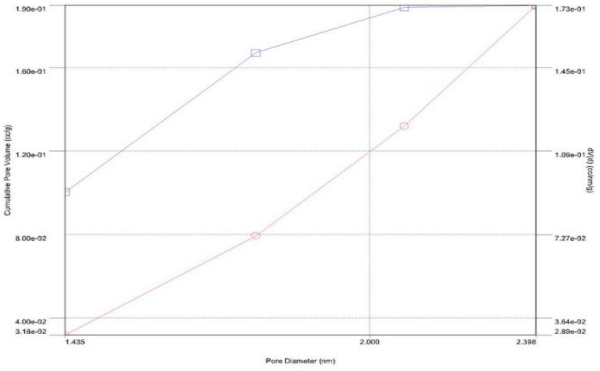

Figure 6: BET Analysis Showing Gradual Increase in Pore Volume with Increasing Pore Diameter

Optimization of Parameters (Dosage, pH, Time and Temperature)

Ampicillin and Paracetamol increased with increasing FeNP dosage, reaching apparent plateaus. For Ampicillin, the optimum dosage was 0.03 g, beyond which no significant improvement in removal was observed (maximum efficiency at 47.5%). For Paracetamol, removal increased steadily across the tested range, with the highest efficiency (56.2%) achieved at the maximum dosage of 0.05 g.

The degradation of both pharmaceuticals was most effective at pH5. The effect of temperature on the degradation efficiency of paracetamol and ampicillin was examined over a temperature range of 30-100 °C. For paracetamol, it was found that an increase in temperature up to 40 °C resulted in an improvement in efficiency from 64% up to 69-70% while that of ampicillin was observed to follow a relatively consistent trend over the range of temperatures.

It was observed that as the reaction time increases for paracetamol, more pollutant molecules interracted with the active catalytic sites on the surface of the nanocatalyst, resulting in a higher degradation efficiency at less time. The steady trend in degradation efficiency for ampicillin indicates that the degradation of this compound occurs at a slower rate compared to paracetamol. Ampicillin contains a β-lactam ring with a more complex molecular structure compared to paracetamol (Zaidi *et al*., 2025).

Degradation Kinetics

The linear relationship between ln(C_0/Ct) and reaction time for both paracetamol and ampicillin signifies that the degradation process carried out by the green-synthesized iron nanocatalyst occurs in pseudo-first-order kinetics.

Pseudo-first-order kinetic equation: ln(C0/Ct) =kt

where:

$C_0 = 50.0$mg/L

C_t= concentration at time t

k= pseudo-first-order rate constant (min^{-1})

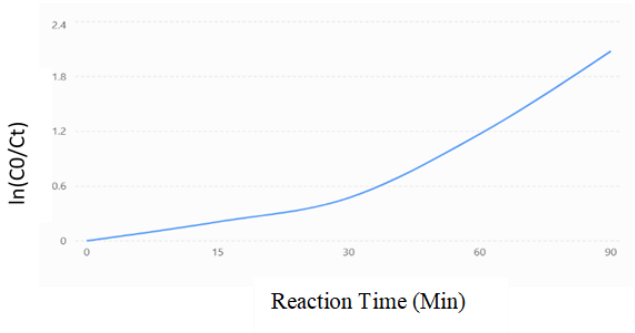

Figure. 7: Percentage Removal and Plot of In(C0/Ct) Versus Time for the Degradation of Paracetamol Using Synthesized FeNPs at Optimized Conditions (0.05g dosage, 80^{0}C and pH 5)

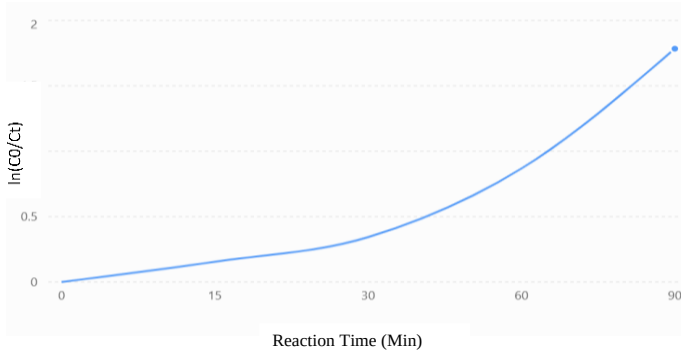

Figure. 8: Percentage Removal and Plot of In(C0/Ct) Versus Time for the Degradation of Ampicillin using Synthesized FeNPs at Optimized Conditions (0.03g dosage, 0^{0}C and pH 5)

The degradation kinetics of the pharmaceutical pollutants was determined by pseudo-first-order kinetic equation plotting ln(C_0/Ct) vs. Reaction Time. Near linear relationship was observed in both cases, which proves that the catalytic degradation process occurred in pseudo-first order kinetics. Rate constants of 0.0232 min^{-1} and 0.0196 min^{-1} were obtained from the two samples where sample one was paracetamol and sample two was ampicillin. Paracetamol degraded faster because of the higher rate constant, which showed high catalytic activity towards paracetamol degradation. The kinetics of degradation noted in the current study are consistent with those found earlier for iron-based nanomaterials. According to the findings of Darma *et al.* (2025), degradation of methyl orange through the photocatalysis effect of the CuO-α-Fe_2O_3 nanocomposite proceeds through a pseudo first order kinetic mechanism.

Arrhenius Plot

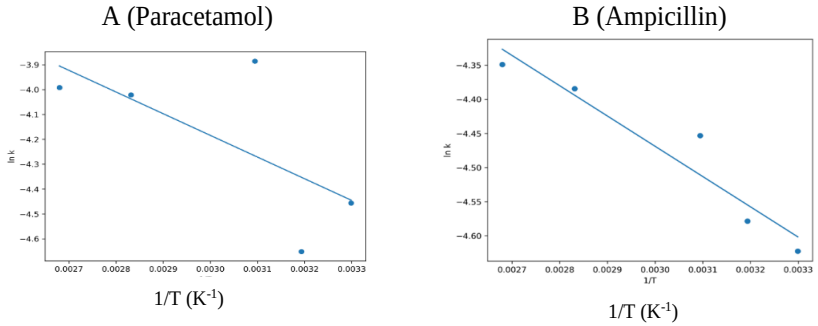

Figure. 9: Arrhenius Plot for the Degradation of Paracetamol (a) and Ampicillin (b) Using FeNP Catalyst

For paracetamol, activation energy is found to be about 5.5 kJ mol^{-1}, which implies that the synthesized iron nanoparticles were efficient in reducing the activation energy for the degradation of paracetamol. This is a sign that the degradation of the drug was catalytically fast. The positive value of the enthalpy change (2.73 kJ mol^{-1}) shows that the reaction is endothermic. The negative value of entropy (-240 J mol^{-1} K^{-1}) reveals that the activated complex formed during the reaction is an ordered one. Positive Gibbs free energy of activation values which increases with temperature are indicative of the energy required to form the activated complex. For ampicillin, the activation energy for the degradation of ampicillin (7.9 kJ mol^{-1}) is slightly higher compared to that calculated for paracetamol (5.5 kJ mol^{-1}), implying that a slightly higher amount of energy is needed to get to the activated stage for ampicillin. Nonetheless, in both cases, the activation energy values are comparatively lower, thus implying that the iron nanoparticles were able to successfully reduce the energy barrier for the degradation process. The positive enthalpy values imply that the degradation processes are mildly endothermic, while negative entropy values show that an ordered activated complex is formed through the process of catalysis. Positive Gibbs free energy of activation values was due to the energy needed to create activated state.

Catalyst Reusability for Ampicillin and Paracetamol Degradation

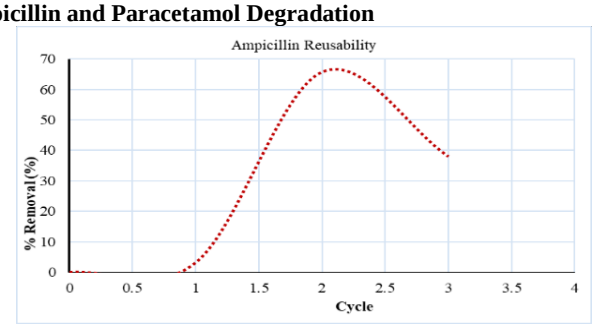

Figure 10: Graph of % Removal VS Cycle for Ampicillin Degradation

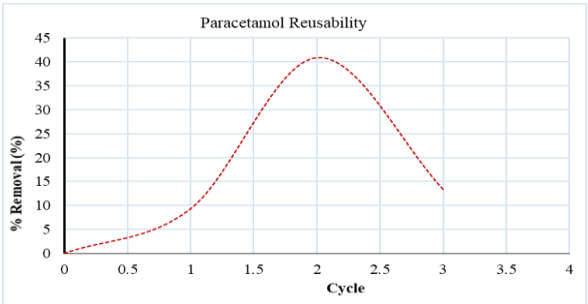

Figure 11: Graph of %Removal VS Cycle for Paracetamol Degradation

It was observed that the rate of increase in degradation efficiency is very high from the first cycle to the second cycle, with the maximum efficiency in the degradation process occurring at 67% (for ampicillin) and 41% for paracetamol in the second cycle. The high increase in the rate of degradation in the first and second cycles can be attributed to the activation of the catalyst's surface in the first cycle, which is a common phenomenon in heterogeneous catalysis, according to Zhang (Zhang *et al*., 2021). However, after the second cycle, the degradation efficiency falls to 40% in the third cycle.

SEM-EDX Analysis of Recycled FeNPs

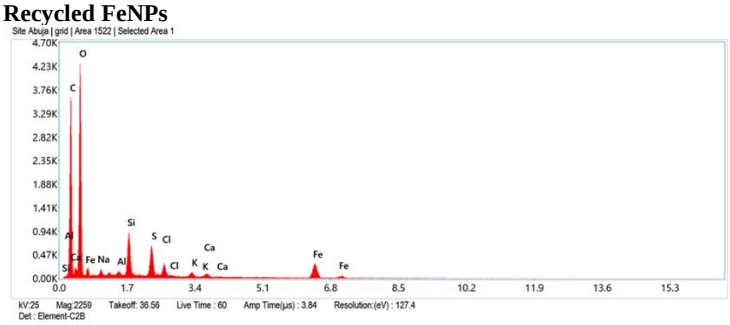

Figure 12: EDX Graph of Recycled FeNPs After Degradation of Pharmaceutical Wastewater

A B

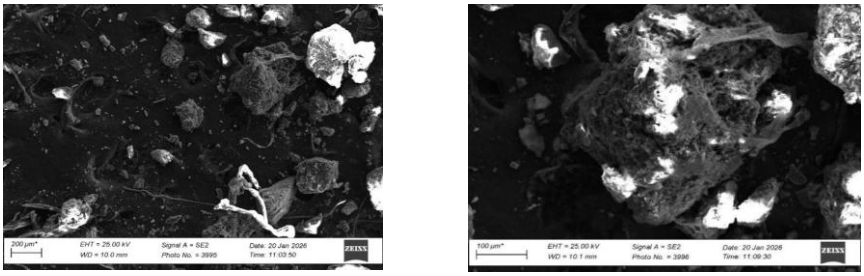

Plate 2 (a&b): SEM Images of Recycled Iron Nanoparticles After Degradation of Pharmaceutical Wastewater

The morphological stability and elemental integrity of the recycled iron nanoparticles after the third degradation cycle were evaluated using Scanning Electron Microscopy (SEM) and Energy Dispersive X-ray Spectroscopy (EDX). Plates 2a and 2b, showed that the nanoparticles are agglomerated, and their surfaces are rough, showing that fusion of nanoparticles and loss of their surface layers have taken place. From the EDX results, it is also confirmed that the nanoparticles are made of iron oxide, and other components such as carbon, oxygen, and silicates are also present, which are from their surfaces after recycling.

Ecotoxicity Results

For the fingerlings, comparison was made across concentrations for survival and behavior. It was observed that some of the fishes in the untreated wastewater were injured, had reduced activity while some died after 48 hours which indicates higher toxic effects.

Mortality was recorded at 24- and 48-hours interval. Fish were considered dead when no movement was observed after gentle prodding.

Calculations: Percentage mortality was calculated.

Mortality (%)} = Number of dead fish/Total number exposed X 100

Secondly, for the algae, physical observation was taken for any decoloration in the algae: There was decoloration of algae in the untreated wastewater compared to the control and the treated wastewater.

Algal growth was measured after 24 h using spectrophotometer

- Measure chlorophyll absorbance at 680 nm.
- Reduced absorbance indicates photosynthetic inhibition

$$\text{Percentage Growth Inhibition (Algae)} = \frac{C.F - S.F}{C.F} \times 100$$

Where C.F= Control fluorescence

S.F= Sample fluorescence

High inhibition= high toxicity while reduced inhibition indicates detoxification success.

CONCLUSION

The synthesized iron nanoparticles were utilized as a catalyst in the degradation of pharmaceutical contaminants in wastewater. The experimental results indicated that the nanoparticles achieved an 88% degradation of paracetamol and 83% degradation of ampicillin under optimized conditions of pH 5 and temperature 80^0C. The degradation of the contaminants occurred based on the operational parameters such as contact time, temperature, catalyst dosage, and pH. From the findings of this research study, it is evident that cassava peel-based iron nanoparticles are effective in the degradation of pharmaceutical wastewater at a minimal cost and in an environmentally friendly manner. The use of agricultural waste such as cassava peel in the synthesis of nanoparticles is not only cost-effective but also environmentally friendly and promotes the concept of green chemistry. Further research in catalyst stability and regeneration studies, and investigation of degradation pathways are recommended to enhance the efficiency of the reaction in wastewater treatment systems.

CONFLICT OF INTEREST

The authors declare no conflict of interest.

REFERENCES

Darma, M. S., Hamza, A., & Imrana, I. (2025). Kinetics of photocatalytic degradation of methyl orange using CuO-α-Fe_2O_3 nanocomposite under visible light irradiation. *FUDMA Journal of Sciences*, 9, 216–223. DOI: https://doi.org/10.33003/fjs-2025-09(AHBSI)-3435

Dutta, V., Sharma, S., & Raizada, P. (2020). Photocatalytic degradation of pharmaceutical pollutants using metal oxide nanomaterials: A review. *Journal of Environmental Chemical Engineering*, 8(5), 104316.

Eche, P. I., Shaibu, S. E., Uwah, E. I., & Moses, E. A. (2025). One-pot biosynthesis and structural elucidation of iron-

biochar nanocomposites from waste coconut shells. *FUDMA Journal of Sciences*, 9(2), 13–22. DOI: https://doi.org/10.33003/fjs-2025-0902-3037

Iravani, S. (2011). Green synthesis of metal nanoparticles using plants. *Green Chemistry*, 13(10), 2638–2650.

Jain, R., Mendiratta, S., Kumar, L., & Srivastava, A. (2021). Green synthesis of iron nanoparticles using Artocarpus heterophyllus peel extract and their application as a heterogeneous Fenton-like catalyst for the degradation of Fuchsin Basic dye. *Current Research in Green and Sustainable Chemistry*, 4, 100086.

Kayode-Afolayan, S. D., Ahuekwe, E. F., & Nwinyi, O. C. (2022). Impacts of pharmaceutical effluents on aquatic ecosystems. Scientific African, 17, e01288.

Khan, I., Saeed, K., & Khan, I. (2022). Green synthesis of iron oxide nanoparticles and their environmental applications. *Environmental Research*, 204, 111967.

Kolawole, A. S., & Iyiola, A. O. (2023). Environmental pollution: threats, impact on biodiversity, and protection strategies. In Sustainable utilization and conservation of Africa's biological resources and environment (pp. 377-409). Singapore: *Springer Nature Singapore*.

Kumar, H., Bhardwaj, K., Sharma, R., Nepovimova, E., & Kuca, K. (2023). Green synthesis of metallic nanoparticles using fruit and vegetable waste: A step towards sustainable waste management. *Journal of Environmental Management*, 344, 118499.

Makarov, V. V., Love, A. J., Sinitsyna, O. V., Makarova, S. S., Yaminsky, I. V., Taliansky, M. E., & Kalinina, N. O. (2014). Green synthesis of metal nanoparticles using plants: A review. *Acta Naturae*, 6(1), 35–44.

Organisation for Economic Co-operation and Development (2011). Test No. 201: Freshwater alga and cyanobacteria, growth inhibition test. *OECD Guidelines for the Testing of Chemicals*, Section 2. OECD Publishing, Paris.

Organisation for Economic Co-operation and Development (2019). *Test No. 203: Fish acute toxicity test*. OECD Guidelines for the Testing of Chemicals, Section 2. OECD Publishing, Paris. https://doi.org/10.1787/9789264069947-en

Rahman, M. S., Hossain, M. M., & Islam, M. A. (2023). Surface area and pore structure effects on catalytic activity of green-synthesized iron oxide nanoparticles. *Journal of Environmental Chemical Engineering*, 11(2), 109876.

Rathod, S. V., Saras, P., & Gondaliya, S. M. (2024). Environmental pollution: Threats and challenges for management. In Eco-restoration of polluted environment (pp. 1-34). CRC Press.

Sharma, G., Kumar, D., Pandey, P., & Singh, A. (2022). Biological synthesis of nanoparticles and their applications in environmental remediation: A sustainable approach. *Environmental Nanotechnology, Monitoring & Management*, 17, 100656.

Singh, J., Dutta, T., Kim, K.-H., Rawat, M., Samddar, P., & Kumar, P. (2018). Plant-mediated synthesis of metal nanoparticles and their environmental applications. *Journal of Nanobiotechnology*, 16, 84.

Singh, R., Kumar, P., & Sharma, V. (2022). Structural properties of green synthesized iron oxide nanoparticles. *Journal of Environmental Chemical Engineering*, 10, 107875.

Zaidi, N., Mir, M. A., Chang, S. K., Abdelli, N., & Andrews, K. (2025). Integrating computational analysis with IR, Raman, and visible spectroscopy for ampicillin characterization. Tropical Journal of Pharmaceutical Research, 24(11).

Zhang, Y., Li, X., & Chen, H. (2021). Influence of pore structure on catalytic performance of iron oxide nanoparticles. *Applied Surface Science*, 563, 150321.